

MASSIVE METASTABLE CHARGED (S)PARTICLES AT THE LHC

ARE R. RAKLEV

*Department of Applied Mathematics and Theoretical Physics, University of Cambridge,
Wilberforce Road, Cambridge CB1 2ET, UK**A.Raklev@damtp.cam.ac.uk*

This brief review deals with recent interest in the prospects of observing a Massive Metastable Charged Particle (MMCP) at the Large Hadron Collider (LHC), and measuring its properties there. We discuss the motivation for scenarios with MMCPs in a phenomenological context, focusing on supersymmetric models that allow us to explore the expected experimental signatures of MMCPs at the LHC. We review current bounds and give estimates of the LHC reach in terms of MMCP masses.

Keywords: Review; metastable; MMCP; supersymmetry; LHC

PACS Nos.: 12.60.Jv, 13.85.Rm, 14.80.Ly

1. Introduction

With the turn-on of the LHC, the High Energy Physics community will have access to energies that have hitherto been un-probed in lab-based experiments. It is then perhaps natural that at this time there is a plethora of ideas for what New Physics might hide at these energies. Three main ideas seem to underpin most of the work currently being done: i) the need for a viable Dark Matter candidate, ii) the want of an explanation of the hierarchy problem in the Standard Model, and iii) the desire for a Grand Unified Theory (GUT).

Solutions to any one of these problems seem to require an extension of the particle content of the Standard Model, and such extensions often predict a rich New Physics sector at the TeV scale. This is not surprising, since both the Weakly Interacting Massive Particle (WIMP) interpretation of Dark Matter and the scale of electro-weak symmetry breaking point to this energy range, if not even lower.

In exploring the TeV scale with the LHC, most suggested New Physics searches focus on the decay products of short-lived resonances. Weakly interacting Dark Matter candidates, assumed stable, appear only as missing energy signatures. However, several mechanisms are known that could result in Massive Metastable Charged

Particles (MMCPs),^a with a broad range of possible lifetimes. The long lifetime for these particles is often intimately connected with the stability of a Dark Matter candidate. The spectacular signatures of such models and their great physics potential, has attracted a lot of attention over the last years. Indeed, the recent popularity of MMCPs is perhaps best gauged by the multitude of names they have been given in the literature: Stable Massive Particles (SMPs), Long-Lived Charged Massive Particles (CHAMPs), Heavy Stable Charged Particles (HSCPs), Charged Massive Stable Particles (CMSPs), and so on.

To focus our discussion within the limited space available in this brief review we will use supersymmetric models to illustrate the most important properties of MMCPs at the LHC. There are certainly many interesting possibilities beyond supersymmetry; a more complete listing of MMCPs candidates, that demonstrate their seemingly ubiquitous nature in New Physics models, can be found in Section 2 of the excellent review by Fairbairn *et al.* given as Ref. 1. Nevertheless, in terms of the expected LHC phenomenology, most other candidates are very similar to one or more supersymmetric MMCPs, with the exception of MMCPs with magnetic charge or fractional electric charges. We will also refrain from any extensive discussion of the cosmological implications of MMCPs, although these do contribute in setting bounds on MMCP properties.

We shall begin this review by looking briefly at possible mechanisms behind the stability of massive particles, exemplified by supersymmetric models that give MMCPs, in Section 2, before we discuss the experimental signatures and issues at colliders in Section 3. We then review the current bounds on sparticle MMCPs in Section 4 and give our expectations for the LHC in terms of the discovery reach and the measurement of MMCP properties in Section 5, before we conclude.

2. Massive Metastable Charged Particles in Supersymmetry

In the Standard Model (SM) we have a wide selection of different types of long-lived particles: the stable elementary — or so we believe — electron, the metastable elementary muon, and (very) long-lived composite particles such as neutrons and protons. These SM particles illustrate very well various possibilities for stability mechanisms:

- (i) Lightest state carrying a conserved quantum number (electron, proton).
- (ii) Suppressed (effective) coupling (muon).
- (iii) Lack of phase space for decay (neutron).

The electron has no lighter electrically charged state in the SM, while the proton, although decays such as $p \rightarrow \pi^0 e^+$ are kinematically allowed, is protected by the

^aBy metastable we mean any particle that is stable on the scale of a lab-based detector experiment, *i.e.* that normally passes through the detector before decaying. The average distance travelled by an MMCP with energy E and mass m before it decays is given by $\gamma c\tau$, where $\gamma = E/m$. Charged particles are in this context electromagnetically charged and/or have strong interactions.

conservation of lepton- and baryon-number. It is interesting to note the different origins of these conservation laws; charge conservation is the result of a local gauge symmetry, while lepton and baryon number are global non-gauge accidental symmetries of the SM that can be broken by higher dimensional operators. Clearly both mechanisms can be used to provide MMCPs in New Physics scenarios.

In the second mechanism metastability comes about through small couplings to kinematically allowed decay products. Very small couplings on their own raises the question of fine tuning in the theory. However, an effective coupling can be small due to large differences in scales between the decaying particle, and some mediator of the decay. This is the case for the muon whose decay proceeds through an effective four-fermion dimension-six operator with coupling $g^2 m_\mu^2 / 8m_W^2$.

Another option is the lack of phase space for an otherwise allowed decay. Again mass degeneracies may seem fine tuned for elementary particles, less so for composite particles that get their mass from the same dynamics. In the SM the neutron decays as $n \rightarrow p^+ e^- \bar{\nu}_e$, where the available kinetic energy of 0.8 MeV to the final state is tiny compared to the neutron mass, giving a very long lifetime. The mass degeneracy between the proton and the neutron is a fortunate consequence of QCD dynamics. Stability mechanisms that are not seen in the SM particle spectrum, have been suggested. Topological defects such as magnetic monopoles and Q-balls are MMCP candidates. These distinguish themselves by the possibility of having much larger charges than other MMCPs.

In the following discussion of supersymmetric MMCPs we will tacitly assume that R-parity is conserved for the scenarios considered unless stated otherwise. This conserved quantum number, corresponding to point (i) above, ensures that sparticles can only decay into other lighter sparticles, resulting in a completely stable Lightest Supersymmetric Particle (LSP), which as a possible Dark Matter candidate needs to be neutral. This also prevents the rapid decay of an MMCP candidate into SM particles.

We can broadly classify all MMCPs on the basis of their electric and colour charges. This distinction will be important for the discussion of collider phenomenology in Section 3. For the $N = 1$ supersymmetric spectrum we find sleptons and charginos in the first class, while the colour charged possibilities are gluinos and squarks. After production, colour charged MMCPs immediately hadronize into so-called R-hadrons with additional quarks and/or gluons, and may or may not acquire an electrical charge in the process. Several models exist in the literature that attempt to describe this hadronization process.^{2,3,4,5} For a colour triplet MMCP the possible composition of the R-hadron is that of a meson- or baryon-like state, *e.g.* the neutral R-meson $\tilde{t}_1 \bar{d}$ or the positively charged R-baryon $\tilde{t}_1 dd$, while a colour octet may also form a glueball-like state with a gluon, $\tilde{g}g$. R-meson production is dominant in current hadronization models, and the equivalence of up- and down-quarks means that roughly half should be charged.

An R-hadron is expected to be surrounded by a small amount of hadronic energy from the hadronization process and QCD radiation from the massive particle,

forming a jet-structure in the direction of the MMCP. However, the energy of the jet is limited in magnitude due to the large mass of the MMCP, and the R-hadron is expected to carry more than 80% of the jet energy in the vast majority of events.¹

Let us now briefly discuss the individual MMCP candidates in supersymmetry. The chargino has mostly been considered in scenarios with Anomaly Mediated Supersymmetry Breaking (AMSB). Here the gaugino masses have a strict hierarchy $|M_2| \ll |M_1| \ll |M_3|$, so that the lightest neutralino, which is the LSP, has a dominant wino component, and the lightest chargino, also dominantly wino, is only marginally heavier. The mass difference is in the sub-GeV range, but due to model constraints it is typically above the pion mass for natural parameter values.^{6,7b} This means that the decay $\tilde{\chi}_1^\pm \rightarrow \tilde{\chi}_1^0 \pi^\pm$ is very important to the collider signature. The chargino decay length $c\tau$ is relatively restricted and lies between 7 cm at 160 MeV mass difference and 1.6 cm at 230 MeV.⁸ For a phenomenological study of a minimal AMSB scenario at the LHC see Ref. 9.

It is of course possible to ignore the supersymmetry breaking motivation and resulting constraints of AMSB in the generic Minimal Supersymmetric Standard Model (MSSM), setting $|M_2| \lesssim |M_1|$ and $|M_2| \ll |\mu|$ by hand at the weak scale to provide a wino LSP, degenerate with the chargino. In this case the mass difference can become even smaller, depending on the parameter tuning, allowing for substantially larger decay lengths dominated by the three-body decay $\tilde{\chi}_1^\pm \rightarrow \tilde{\chi}_1^0 e^\pm \nu_e$. These are easily hundreds of meters when the mass difference is less than the pion mass, making the chargino appear stable in the LHC detectors. Another option for a chargino MMCP is to have $M_{1,2} \gg |\mu|$, giving a degenerate higgsino LSP and chargino, which can even be realised in the focus-point region of the Constrained Minimal Supersymmetric Standard Model (CMSSM). When we later discuss the LHC discovery potential for a chargino MMCP, we will differentiate between the wino and higgsion cases.

In scenarios with Gauge Mediated Symmetry Breaking (GMSB) and in supergravity (SUGRA) inspired models, the gravitino may be the LSP. Any sfermion Next-to-Lightest Supersymmetric Particle (NLSP) has no choice but to decay to the gravitino, and may thus naturally be metastable due to the small effective coupling to the gravitino. For GMSB the suppression is given by $\sqrt{\langle F \rangle}$, the effective supersymmetry breaking scale, and may be as low as 10 – 100 TeV. In SUGRA models the suppression is set by the reduced Planck mass $M_P = 2.4 \cdot 10^{18}$ GeV. This leads to a great range of possible decay lengths for a sfermion NLSP. In GMSB scenarios this has been estimated as,¹⁰

$$c\tau_{\tilde{f}} = 10^{-2} \left(\frac{100 \text{ GeV}}{m_{\tilde{f}}} \right)^5 \left(\frac{\sqrt{\langle F \rangle}}{100 \text{ TeV}} \right)^4 \text{ cm}, \quad (1)$$

^bThe mass difference in the pure wino case can be thought of as the difference between the charged and neutral wino self-energies, which should be $\mathcal{O}(\alpha m_W)$.

which, considering realistic values of $\sqrt{\langle F \rangle}$ and sfermion masses, gives decay lengths from sub-micron to multi-kilometre. The main upper bounds on $\sqrt{\langle F \rangle}$ are of cosmological origin. To avoid ruining Big Bang Nucleosynthesis (BBN) the sfermion lifetime should be less than 10^4 s. This implies that $\sqrt{\langle F \rangle} \lesssim 10^9$ GeV. For a recent evaluation of the bounds see Ref. 11. For Planck scale supersymmetry breaking one arrives at a similar result with the substitution $\langle F \rangle \rightarrow \sqrt{3}m_{3/2}M_P$ in Eq. (1).

Third generation sfermions are usually lighter than the two first due to RGE running effects from a common mass at some high GUT scale, and as a consequence tend to work better as MMCP candidates in models with GUT unification of masses. For a given sfermion flavour \tilde{f} , it is similarly the lightest of the states, \tilde{f}_1 , generally a mixing of the left- and right-handed sfermion, that works as an MMCP. However, given mass degeneracy between the NLSP candidates, several particles may become metastable, and models that are less restricted at GUT scale may provide different flavors for the NLSP. Still, this means that it is the lightest stop, sbottom and stau that are most commonly considered as MMCPs in the literature. In Gravitino Dark Matter (GDM) scenarios the stau is typically the NLSP for small m_0 , giving $m_{\tilde{\tau}_1} < m_{\tilde{\chi}_1^0}$, a region otherwise disallowed due to a charged LSP. If, in addition to small m_0 , we take small $\tan(\beta)$ and large $|A_0|$, the NLSP may be the stop, while large $\tan(\beta)$ and $|A_b| \gg |A_t|$, gives small sbottom masses.

The NLSP mass degeneracy to a neutralino, or even sneutrino, LSP may also provide MMCP candidates. However, the needed mass parameters tend to be fairly fine tuned and unmotivated. Some motivation can be found in a mass degeneracy that is simultaneously used to explain the measured Dark Matter density through co-annihilation of LSP and NLSP. Unfortunately the small mass differences needed for metastability tend to give too large co-annihilation cross sections and consequently too little Dark Matter. For a stop NLSP the situation is a little better because the lifetime of the main decay modes $\tilde{t}_1 \rightarrow c\tilde{\chi}_1^0$ and $\tilde{t}_1 \rightarrow bff'\tilde{\chi}_1^0$ are suppressed by loop-factors and a four-body phase space, respectively.

The final MMCP candidate we will discuss here is the gluino. In GDM scenarios the gluino can clearly be metastable like all other sparticles, if for some reason M_3 is small compared to the other supersymmetry breaking masses so that the gluino is the NLSP, but perhaps more interesting is the split-SUSY scenario where the scalars — except the lightest Higgs that decouples — are much heavier than the gauginos. This ignores the Higgs mass hierarchy problem, but naturally suppresses CP violation and avoids constraints from flavor physics. Since the gluino can only decay through virtual squarks, either to two quarks and a gaugino, or in a loop-decay to a gluon and neutralino, the decay is suppressed by the mass ratio $m_{\tilde{g}}^2/m_{\tilde{q}}^2$, giving the scaling behaviour,^{12,13}

$$c\tau_{\tilde{g}} = 10^{11} \left(\frac{1 \text{ TeV}}{m_{\tilde{g}}} \right)^5 \left(\frac{m_{\tilde{q}}}{10^9 \text{ GeV}} \right)^4 \text{ cm.} \quad (2)$$

The CMSSM focus-point region with sufficiently large values for m_0 displays these properties, but the constraint on electro-weak symmetry breaking means that $m_{1/2}$

must also be rather large, and the sparticle mass spectrum might be outside of the reach of the LHC.

With non-zero R-parity violating couplings the LSP will eventually decay unless it is very light. If the LSP is the gravitino it may still live long enough to constitute Dark Matter.^{14,15,16} For couplings less than $\mathcal{O}(10^{-6})$, the exact value depending on sparticle mass and flavor of the coupling, the lifetime of stable or metastable sparticles is not shortened enough for them to decay inside a detector, and thus has no direct influence on the collider phenomenology of MMCPs. However, a new and interesting possibility opens up: the LSP may well be charged if it has a short lifetime on cosmological scales. This allows for less fine-tuning for many MMCP candidates discussed above that formerly decayed to the LSP, they now simply need to be the lightest sparticle.

3. Experimental Issues

The signatures of MMCPs traversing a detector are determined by their interactions with the matter of the detector. The main source of energy loss for electrically charged massive particles with large velocities, $\beta\gamma \gtrsim 0.1$, is ionisation energy loss through the removal of electrons from atoms in the material. For a particle of velocity $\beta\gamma$ this is given by the Bethe-Bloch formula for mean rate of ionisation energy loss, or stopping power,¹⁷

$$\left\langle -\frac{dE}{dx} \right\rangle = \frac{Kz^2Z}{A\beta^2} \left(\frac{1}{2} \ln \frac{2m_e c^2 \beta^2 \gamma^2 T_{\max}}{I^2} - \beta^2 - \frac{\delta}{2} \right), \quad (3)$$

where $K = 4\pi N_A r_e^2 m_e c^2$. The physical constants and properties of the material and particle involved are: the electric charge z of the particle, the atomic number Z and mass A of the material, the classical electron radius r_e and mass m_e , Avogadro's number N_A , the maximum kinetic energy that can be given to a free electron in a single collision T_{\max} , and the mean ionisation potential of the material I .^c

The δ term in Eq. (3) is a function of velocity that corrects for density effects at relativistic velocities, $\beta\gamma \gtrsim 3$. In addition to the ionisation energy loss, lighter charged particles also have significant radiative losses at high velocities. For muons radiative effects reach 1% at around 10 GeV energy. However, this is mass dependent, and should be insignificant for masses not already ruled out for MMCPs.

From Eq. (3) one finds a minimum around $\beta\gamma \simeq 3$, roughly independent of material and particle mass, for masses much greater than the electron mass. Such a particle is usually termed a minimum ionising particle or mip. The asymptotic behaviour $dE/dx \propto \beta^{-2}$ of the Bethe-Block formula at low velocities is tempered for velocities less than the bound electron velocity, of the order of a few percent of c , where the energy loss is simply proportional to β .

^cNote that x takes the form of length times density of the material and the units are given by $K/A = 0.307075 \text{ MeV g}^{-1} \text{ cm}^2$ for an atomic mass of $A = 1 \text{ g mol}^{-1}$.

The fact that the ionisation energy loss of a charged particle is almost independent of the particle's mass, but dependent on its velocity is crucial in searches for MMCPs at colliders. Firstly, it means that the MMCPs will appear as a muon-like objects in detectors and their momenta can be reconstructed by a tracking system that relies on ionisation energy deposits. Secondly, while the energy loss of an MMCP produced may very well be that of a mip, an accompanying measurement of the particle's momentum p from the curvature of its track in a magnetic field will reveal that the mass m is large since $m = p/\beta\gamma$, and as we have seen above, a measurement of dE/dx fixes the velocity modulo fluctuations in single measurements.

For strong interactions of MMCPs with detector material the situation is much less well understood as we lack sufficiently similar SM counterparts. Several models have been proposed that attempt to describe the scattering of R-hadrons on atomic nuclei.^{2,3,4,5,18,19} The common feature of these models is the spectator nature of the MMCP. Its interactions with partons in the nuclei are suppressed relative to those of the light constituents of the R-hadron by the square of the MMCP mass. The implication is that an R-hadron's properties are largely determined by its light-quark/gluon components.

Despite the spectator role of the MMCP it carries the majority of the R-hadron momentum since the relative momentum of the interacting system is given by the ratio of its mass to the total R-hadron mass. Thus, for an MMCP mass of $\mathcal{O}(100 \text{ GeV})$ or above, the momentum of the scattering system is maximally a few GeV at the LHC. The low-energy scatters means that the energy loss per interaction is also limited, of the order of 1 GeV over a large spectrum of β . While the energy loss to strong interactions is still expected to dominate at high velocities, the rise in ionisation energy loss below the mip velocity means that it dominates at low velocities.

One important consequence of the limited energy loss is that most strongly interacting MMCPs are expected to penetrate large detectors, their tracks, if charged, being in effect reconstructed as muons. The additional complication with R-hadrons is that they may flip charge in inelastic scattering off nuclei, interchanging their non-MMCP partons with those of the nuclei. Thus R-hadron tracks in detectors can be stubs that end or appear abruptly in the tracking system. Recently it has also been shown that R-mesons will tend to convert into R-baryons due to scatterings of the type $R_{\bar{g}q\bar{q}} + N \rightarrow R_{\bar{g}qq} + \pi$ that are energetically favoured, and where the reverse reaction is suppressed due to a lack of pions in the detector material.⁵

The second staple of MMCP searches is the Time-of-Flight (ToF) measurement. With the use of high magnetic fields it is safe to assume that any stable or metastable SM particles reconstructed by a tracking system travel with a velocity of $\beta \simeq 1$. Despite this, due to the large size of modern detector experiments, the ToF from the interaction point and out of the detector can be of $\mathcal{O}(100 \text{ ns})$. Given a time resolution in the nanosecond range, particle velocities can then be reconstructed with good precision. Since massive particles are produced with much smaller velocities, these can be discriminated from SM backgrounds, and again the combination of momentum and velocity measurements leads to a measurement of the mass.

While the low velocity of the MMCPs is an advantage for measuring masses, it poses serious challenges for triggering on signal events and the acquisition of data in modern high luminosity colliders. This is particularly true for the LHC, where the distance between two bunch crossings (BCs) is only 25 ns at design luminosity. This corresponds to 7.5 m at light-speed, meaning that up to three BCs are simultaneously contained inside the large ATLAS and CMS detectors. This is taken into account in detector design and read-out, however, assuming particle velocities near c . Slower particles may cause triggers to be assigned to the wrong BC, or the MMCP not to be recorded in the triggered BC.²⁰ Simple estimates from ATLAS geometry give that MMCPs with $\beta > 0.7$ reach the outer parts of the muon trigger system inside the correct BC.²¹ This is confirmed in a full simulation study of MMCPs that show large efficiencies for hits in the muon trigger chambers at $\beta \gtrsim 0.7 - 0.8$ with standard trigger windows.^{22,23} If MMCPs are indeed discovered at the LHC, trigger windows can be enlarged to values used in calibration and debugging to improve efficiencies and reach lower velocities.

For the particular case of R-parity conserving supersymmetric models, MMCPs are produced in pairs at colliders, either through cascade decays or direct production. This means that there are at least two possible muon trigger objects in each event, which improves the final trigger efficiency, in particular for cascade decays where the MMCPs may be produced with wildly different velocities. The exception is the R-hadron scenario, where one or both of the R-hadrons may be neutral by the time they pass through the muon system, either from being produced neutral or by charge flipping interactions.

The second difficulty with slow moving MMCPs is the drop in track reconstruction efficiency. Tracking software also operates under the $\beta = 1$ assumption, so that slow particles typically have a bad quality of fit for their tracks and may be discarded, *e.g.* for the Monitored Drift Tubes (MDTs) in the ATLAS muon system, hits from slower particles are assigned too large drift distances from the tube centre so that the reconstruction is attempted with mismeasured coordinates. As a result the reconstruction efficiency is found to decrease dramatically below $\beta = 0.75$.^{21,22,23} The solution suggested in Ref. 24 is to keep β a free parameter of the fit and maximise the fit quality over β . This simultaneously allows for better reconstruction efficiencies and a determination of the MMCP velocity. In a full simulation study, using also information from the timing of hits in the muon trigger system and recovering trigger hits from the next BC, Ref. 22 finds good reconstruction efficiencies down to $\beta \simeq 0.5$.

4. Current Constraints

The best current collider bounds on MMCP cross sections and masses originate from the OPAL experiment at LEP and recent results published by the Tevatron CDF and D0 experiments.^{25,26,27} The lower mass bounds are typically the result of a comparison between the predicted pair-production cross section of an MMCP in a

particular model, and a limit on the number of events with particles reconstructed above a certain mass from the experiment. Below we review these bounds and comment briefly on the assumptions going into them. In general, the reliance on pair-production cross sections gives conservative mass bounds for sparticle MMCP candidates, with little or no model dependence. If interpreted in specific constrained models, the Tevatron bounds can improve dramatically, in particular for weakly interacting sparticles, where the dominant production is expected to be from the decays of strongly interacting sparticles with much higher cross sections.

The OPAL experiment uses a measurement of dE/dx for each track compared to the momentum to distinguish massive charged particles from SM backgrounds. The ionisation energy loss is measured with a good resolution of 2.8%, using multiple, above 20 required, hits on sense wires in the OPAL jet chamber. The results are based on data collected at centre-of-mass energies from 130 GeV to 209 GeV, with a total integrated luminosity of 693.1 pb⁻¹. In the absence of any signal, a 95% C.L. bound on the pair-production cross section of weakly interacting MMCPs is given in terms of the MMCP mass and spin, assuming s -channel production. Translated into sparticle masses this implies a lower limit of 98.0 GeV and 98.5 GeV on right- and left-handed sleptons, respectively, for smuons and staus. Note that this bound does not translate to selectrons, as their cross section depends on other sparticle parameters in t -channel production. The same model-dependence is also present for chargino pair-production in terms of the wino-higgsino mixing and the sneutrino mass. By minimising the chargino cross section over the CMSSM parameter space for a fixed chargino mass, a lower limit of 102.0 GeV is found.

For squark MMCPs the ALEPH experiment at LEP has given direct mass bounds, with the conservative assumption that stop and sbottom mixing angles are such that their couplings to the Z disappear.²⁸ The resulting lower limits on the lightest mass eigenstates are $m_{\tilde{t}_1} > 95$ GeV and $m_{\tilde{b}_1} > 92$ GeV at 95% C.L. For a gluino MMCP, the bounds from LEP are much weaker. The dominant production process is $e^+e^- \rightarrow q\bar{q}\tilde{g}\tilde{g}$, where a gluon radiating off one of the quarks splits into two gluinos. The ALEPH collaboration gives a bound of $m_{\tilde{g}} > 26.9$ GeV.²⁸

The Tevatron CDF experiment reports complementary bounds for weakly interacting MMCPs and more stringent bounds for strongly interacting MMCPs set with 1 fb⁻¹ of data at $\sqrt{s} = 1.96$ TeV. The CDF experiment uses a ToF detector to measure the masses of particles with high transverse momentum in a sample of events collected with the muon trigger. Standard Model backgrounds are estimated from the mass resolution on muon-like particles found in a control-region, and no excess of events is found for masses above 100 GeV. Along with an evaluation of the signal efficiency, this allows fully model independent cross section bounds of $\sigma < 10$ fb and $\sigma < 48$ fb to be set on weakly and strongly interacting MMCPs, respectively, for a single MMCP within the experimental cuts of $p_T > 40$ GeV, $|\eta| < 0.7$, $0.4 < \beta < 0.9$ and $m > 100$ GeV. Note that the CDF analysis does not consider the R-meson to R-baryon transition mentioned in Section 3 when evaluating the signal efficiency. The R-baryon should have a larger interaction cross section, leading to lower efficiency,

so that the final mass limit may be slightly overestimated.

For an interpretation of these bounds in terms of sparticle masses, the differential pair-production cross sections need to be evaluated and integrated over the acceptance region. This was done for a stop MMCP candidate, yielding a lower bound of $m_{\tilde{t}_1} > 249$ GeV at the 95% C.L. for a specific supergravity inspired scenario where the other squark masses are set to $m_{\tilde{q}} = 256$ GeV, the gluino mass $m_{\tilde{g}} = 284$ GeV and the stop mixing angle $\sin(2\theta) = -0.99$. However, the stop pair-production cross section at NLO is known to be rather insensitive to these parameters, see Ref. 29. We evaluate this effect using PROSPINO 2.1,^{29,30,31} decoupling the contribution from gluinos and other squarks by setting their masses to 2 TeV and minimising the cross section over the mixing angle. As expected, this gives only a slightly softer bound of $m_{\tilde{t}_1} > 247.5$ GeV.

No explicit mass limits for other supersymmetric MMCPs were found in Ref. 26. For the gluino in particular the CDF data should result in an improvement of the LEP mass limit, and its evaluation would be feasible with Monte Carlo simulation of the kinematics of gluino pair-production and a re-evaluation of the signal efficiency for a gluino based R-hadron. Similar considerations apply to the sbottom, where the cross section should be identical to the stop's in the decoupling limit, but where the signal efficiency for an R-hadron containing a down-squark could be different due to the preferred formation of a neutral R-baryon.

The D0 experiment presents a similar analysis using 1.1 fb^{-1} of data, measuring particle velocity through ToF with timing from scintillation trigger counters in the muon system. The results are less model independent in that they are interpreted directly in terms of upper cross section bounds on the pair-production of staus and charginos. For the stau, no mass limit can be set as the predicted cross section is too low. For the chargino, mass limits of 206 GeV and 171 GeV, for a wino- and higgsino-like chargino, respectively, is given at the 95% C.L.

We give a summary of the best limits discussed above in Table 1. In addition to these bounds there are also indirect bounds such as the measurement of the invisible Z width, which constrains the mass of supersymmetric MMCPs that couple to the Z to be above $m_Z/2$, and the running of α_s , which limits colour charged particles beyond the SM to have masses greater than about 6 GeV.³² While these limits are less constraining than the direct bounds discussed above, they have the advantage of closing low-mass loopholes in the direct bounds. As mentioned in Section 2 there are also limits on the MMCP lifetime from cosmology that translate to mass limits, given model dependent assumptions on couplings and/or other sparticle masses.

5. LHC Prospects

With the large increase in centre-of-mass energy from the Tevatron to the LHC, the LHC experiments will naturally be sensitive to more massive MMCPs. We begin this Section with a discussion of the prospects for applying dE/dx and ToF techniques to discovering MMCPs and measuring their masses in the large LHC experiments.

Table 1. Summary of current best limits on MMCP masses in supersymmetry.

| MMCP | Mass limit [GeV] | Notes | Source |
|----------------------|------------------|--|----------------|
| $\tilde{\chi}_1^\pm$ | 206.0 | Assuming $\tilde{\chi}_1^\pm \simeq \tilde{W}^\pm$. | D0, Ref. 27 |
| | 171.0 | Assuming $\tilde{\chi}_1^\pm \simeq \tilde{H}^\pm$. | D0, Ref. 27 |
| $\tilde{\ell}_1$ | 98.0 | $\tilde{\ell} = \tilde{\mu}, \tilde{\tau}$, assuming $\tilde{\ell}_1 \simeq \tilde{\ell}_R$. | OPAL, Ref. 25 |
| | 98.5 | $\tilde{\ell} = \tilde{\mu}, \tilde{\tau}$, assuming $\tilde{\ell}_1 \simeq \tilde{\ell}_L$. | OPAL, Ref. 25 |
| \tilde{g} | 26.9 | Could be improved using Tevatron data. | ALEPH, Ref. 28 |
| \tilde{t}_1 | 247.5 | Re-evaluated in this review. | CDF, Ref. 26 |
| \tilde{b}_1 | 92.0 | Could be improved using Tevatron data. | ALEPH, Ref. 28 |

We then show an estimate of the discovery reach of the LHC in terms of sparticle MMCP masses, before we touch on the exciting possibility of stopped MMCPs.

In both ATLAS and CMS the principal sub-detectors for measuring dE/dx are in the inner tracking systems. Although more energy will be deposited in the calorimeters, a reliable determination of dE/dx needs several measurements on account of large fluctuations. In published ATLAS results the current optimal strategy uses a measurement of the time a hit in the Transition Radiation Tracker (TRT) is over an ionisation threshold.³³ This is strongly correlated with dE/dx and can be used on slow particles, $\beta \lesssim 0.7$, where from the Bethe-Bloch formula we have $dE/dx \propto \beta^{-2}$. Results given in Ref. 34 indicate that in this region a resolution on the velocity of somewhat better than 20% is achievable. For CMS, the inner tracking system consists of silicon pixel and silicon strip detectors, the dE/dx resolution of these devices is somewhat worse than for gaseous detectors such as the ATLAS TRT.

Assuming that the error on the momentum and velocity measurements are uncorrelated, the mass resolution is given by

$$\left(\frac{\sigma_M}{M}\right)^2 = \left(\frac{\sigma_p}{p}\right)^2 + \left(\gamma^2 \frac{\sigma_\beta}{\beta}\right)^2. \quad (4)$$

As expected the resolution becomes very bad for $\beta \rightarrow 1$. With a typical transverse momentum resolution of 4 – 10% for the 100 GeV to 1 TeV momentum range in ATLAS,³⁵ we see that the mass resolution is dominated by the β -resolution. Thus a 20% resolution on the MMCP mass should realistically be achievable in ATLAS using the time-over-threshold technique.

For a mass measurement using ToF, the error in the velocity measurement is dominated by the timing resolution since the positions of hits inside a detector will be very well known from an extensive calibration programme. Thus we can substitute $\sigma_\beta/\beta = \sigma_t/t$ in Eq. 4. From a simple order of magnitude estimate, using the size of a generic LHC detector and a 1 ns fluctuation on the time measurement, we get a resolution of $\sigma_t/t \simeq 0.02$, showing the advantage of the size of the LHC detectors. This matches well with various full simulation studies of the ATLAS detector using the track re-fit method described in Section 3, timing information from the muon trigger system, or both.^{21,22,23,24,36} These arrive at similar resolutions of

$\sigma_\beta/\beta = 0.02 - 0.03$ for a stau MMCP, which is competitive with the contribution to the mass resolution from the momentum measurement at low velocities ($\beta \lesssim 0.8$).

The final precision with which the MMCP mass can be determined is of course to some degree dependent on the available statistics, the MMCP mass, and to an extent on whether the MMCP has electric and/or colour charge.^d However, the good resolution achievable with ToF techniques quickly reduces the statistical error to below 1 GeV, so that the mass determination is dominated by systematic errors that have been found to be around 1 – 2 GeV in Monte Carlo simulations.^{21,22} This level of precision has been shown to allow the efficient reconstruction of many heavier sparticles, if not too heavy to be produced, that decay into the MMCP, giving precise access to a large fraction of the sparticle spectrum.³⁷

At present little has been published by the LHC experiments on their potential discovery reach in terms of MMCP masses; exceptions are found in Refs. 23, 33 and 39. This is understandable as potential main backgrounds such as muons with misreconstructed velocities are difficult to estimate from Monte Carlo alone, without the benefit of the detector understanding that comes with data. Nevertheless, we can attempt a rough estimate of the LHC reach under the assumption that an MMCP search at the LHC will be a low background search, with $\mathcal{O}(1)$ background events expected for some fixed integrated luminosity and a corresponding signal efficiency; this is based on similar analysis at the Tevatron and at LEP, described in Section 4.

We adopt a fairly conservative guess for the signal efficiency of 20% and 5%, for weakly interacting and strongly interacting MMCPs, respectively, based on CMS numbers for a search with first data.³⁹ With the NLO pair-production cross sections computed by PROSPINO 2.1 in the limit where other sparticles effectively decouple, we show the integrated luminosity needed for “discovery” as a function of MMCP mass in Fig. 1. The required luminosity is of course dependent on the expected number of background events for a given luminosity, and we have assumed $B = 1$ for 100 pb^{-1} , but the required luminosity scales linearly with B if one takes S/\sqrt{B} as the significance. In the same way the interested reader can easily re-scale Fig. 1 to a different signal efficiency, since the required integrated luminosity scales as ϵ^{-2} .

While the above discussion has focused mostly on properties of the ATLAS detector, the situation for CMS is similar, with somewhat better signal efficiencies expected due to its “compact” design, and a somewhat worse mass resolution for the same reason.^{38,39,40} For the smaller experiments work on MMCPs has been limited, but it is possible that the LHCb detector may be competitive in some areas of parameter space due to excellent particle identification properties. The LHCb will certainly be in a good position to observe long-lived particles decaying inside the detector, a topic which is outside the scope of this paper. In addition, the MOEDAL experiment has proposed to search for highly ionising exotic particles such as magnetic monopoles and Q-balls, through the use of a passive plastic track-

^dBecause of interactions with nuclei, R-hadrons lose more energy in the calorimeters. Charge flipping also makes precise momentum and velocity determination more difficult.

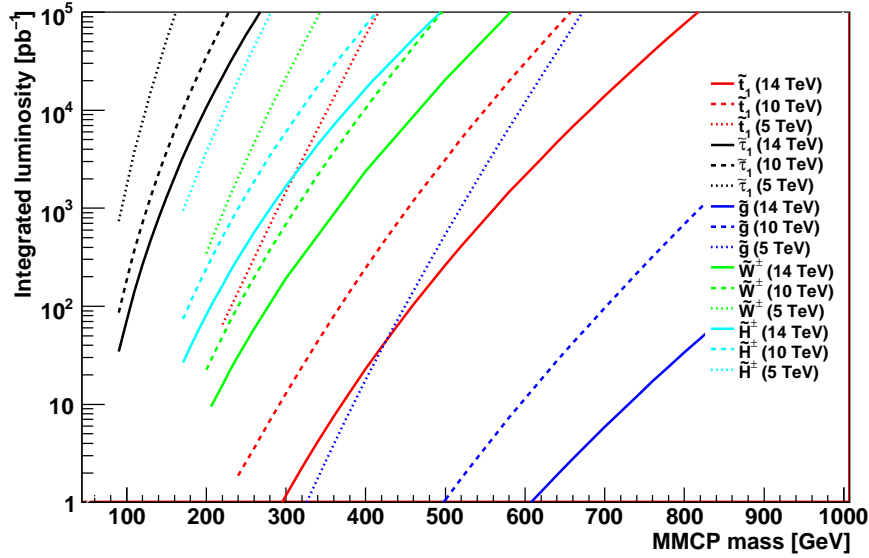


Fig. 1. Integrated luminosities needed for discovery versus MMCP mass for the LHC at 14 TeV (solid), 10 TeV (dashed) and 5 TeV (dotted). The colours denote different sparticle species: stop (red), stau (black), gluino (blue), charged wino (green) and higgsino (cyan).

etch detector surrounding the LHCb vertex detector.⁴¹

Finally in this Section, we want to mention a very interesting possibility due to MMCP energy loss: MMCPs produced with small momenta may lose enough energy to ionisation to be stopped inside the detector, most probably inside a calorimeter, or in a dedicated stopper detector as suggested in Refs. 42, 43 and 44. Due to the small energy losses expected the fraction of stopped MMCPs will be a small unless the MMCP is very heavy, in which case the small cross section limits the number of stopped MMCPs. Even if rare, stopped MMCPs may open up a very exciting new direction of exploration: that of detecting late decays of MMCPs, with lifetimes from a fraction of a second to years. This idea has already seen initial exploration at the Tevatron D0 experiment, looking for stopped gluinos.^{45,46}

Decays in the detector out of sync with collisions, or even with no beam present, will enable a measurement of the MMCP lifetime and its dominant decay channel(s), if the decays can be separated from cavern backgrounds and cosmic ray hits, and enough statistics is available. In models with a gravitino LSP the gravitino mass could also be measured given knowledge of the MMCP mass and the recoil energy against an invisible gravitino in the MMCP decay. The implication of all this is that the coupling of the MMCP to the gravitino will be indirectly determined from the MMCP lifetime, which constitutes a microscopic measurement of Newton's constant, and a powerful piece of evidence in favour of supergravity.⁴⁷

6. Conclusion

We have given a brief review of the prospects for discovering Massive Metastable Charged Particles at the LHC, focusing on supersymmetric scenarios. The unprecedented centre-of-mass energy of the LHC allows mass scales far above current constraints to be probed even with limited statistics. The discovery of such a particle will herald a revolution in particle physics: measuring the properties of the MMCP will give clear indications of the structure of physics beyond the Standard Model, in the same way that the properties of stable and metastable Standard Model particles have helped reveal the structure of that model.

The general purpose LHC detectors are well suited to measure the mass and charge of an MMCP as a result of their size and the excellent timing and momentum resolution in several sub-detectors. If stopped in the detectors, the MMCP lifetime can also be determined, with possible implications even for Planck scale physics.

Acknowledgments

ARR acknowledges funding from the UK Science and Technology Facilities Council (STFC) and wishes to thank John R. Ellis and Ola K. Øye for fruitful collaborations on this topic, as well as David A. Milstead and members of the Cambridge Supersymmetry Working Group for many interesting and helpful discussions.

References

1. M. Fairbairn, A. C. Kraan, D. A. Milstead, T. Sjostrand, P. Skands and T. Sloan, Phys. Rept. **438**, 1 (2007) [arXiv:hep-ph/0611040].
2. M. Drees and X. Tata, Phys. Lett. B **252** (1990) 695.
3. H. Baer, K. M. Cheung and J. F. Gunion, Phys. Rev. D **59** (1999) 075002 [arXiv:hep-ph/9806361].
4. A. Mafi and S. Raby, Phys. Rev. D **62** (2000) 035003 [arXiv:hep-ph/9912436].
5. A. C. Kraan, Eur. Phys. J. C **37** (2004) 91 [arXiv:hep-ex/0404001].
6. J. L. Feng, T. Moroi, L. Randall, M. Strassler and S. f. Su, Phys. Rev. Lett. **83** (1999) 1731 [arXiv:hep-ph/9904250].
7. T. Gherghetta, G. F. Giudice and J. D. Wells, Nucl. Phys. B **559** (1999) 27 [arXiv:hep-ph/9904378].
8. C. H. Chen, M. Drees and J. F. Gunion, arXiv:hep-ph/9902309.
9. A. J. Barr, C. G. Lester, M. A. Parker, B. C. Allanach and P. Richardson, JHEP **0303** (2003) 045 [arXiv:hep-ph/0208214].
10. G. F. Giudice and R. Rattazzi, Phys. Rept. **322** (1999) 419 [arXiv:hep-ph/9801271].
11. F. D. Steffen, JCAP **0609** (2006) 001 [arXiv:hep-ph/0605306].
12. M. Toharia and J. D. Wells, JHEP **0602** (2006) 015 [arXiv:hep-ph/0503175].
13. P. Gambino, G. F. Giudice and P. Slavich, Nucl. Phys. B **726** (2005) 35 [arXiv:hep-ph/0506214].
14. F. Takayama and M. Yamaguchi, Phys. Lett. B **485** (2000) 388 [arXiv:hep-ph/0005214].
15. W. Buchmuller, L. Covi, K. Hamaguchi, A. Ibarra and T. Yanagida, JHEP **0703** (2007) 037 [arXiv:hep-ph/0702184].

16. S. Lola, P. Osland and A. R. Raklev, Phys. Lett. B **656** (2007) 83 [arXiv:0707.2510 [hep-ph]].
17. C. Amsler *et al.* [Particle Data Group], Phys. Lett. B **667** (2008) 1.
18. R. Mackeprang and A. Rizzi, Eur. Phys. J. C **50** (2007) 353 [arXiv:hep-ph/0612161].
19. Y. R. de Boer, A. B. Kaidalov, D. A. Milstead and O. I. Piskounova, J. Phys. G **35** (2008) 075009 [arXiv:0710.3930 [hep-ph]].
20. S. Bressler, E. Duchovni, L. Levinson and S. Tarem, ATL-PHYS-PUB-2005-022.
21. J. R. Ellis, A. R. Raklev and O. K. Øye, ATL-PHYS-PUB-2007-016.
22. S. Tarem, S. Bressler, H. Nomoto and A. Di Mattia, Eur. Phys. J. C **62** (2009) 281.
23. G. Aad *et al.* [ATLAS Collaboration], arXiv:0901.0512 [hep-ex].
24. G. Polesello and A. Rimoldi, ATL-MUON-99-006.
25. G. Abbiendi *et al.* [OPAL Collaboration], Phys. Lett. B **572** (2003) 8 [arXiv:hep-ex/0305031].
26. T. Aaltonen *et al.* [CDF Collaboration], arXiv:0902.1266 [hep-ex].
27. V. M. Abazov *et al.* [D0 Collaboration], Phys. Rev. Lett. **102** (2009) 161802 [arXiv:0809.4472 [hep-ex]].
28. A. Heister *et al.* [ALEPH Collaboration], Eur. Phys. J. C **31** (2003) 327 [arXiv:hep-ex/0305071].
29. W. Beenakker, M. Kramer, T. Plehn, M. Spira and P. M. Zerwas, Nucl. Phys. B **515** (1998) 3 [arXiv:hep-ph/9710451].
30. W. Beenakker, R. Hopker, M. Spira and P. M. Zerwas, Nucl. Phys. B **492** (1997) 51 [arXiv:hep-ph/9610490].
31. W. Beenakker, M. Klasen, M. Kramer, T. Plehn, M. Spira and P. M. Zerwas, Phys. Rev. Lett. **83** (1999) 3780 [Erratum-ibid. **100** (2008) 029901] [arXiv:hep-ph/9906298].
32. F. Csikor and Z. Fodor, Phys. Rev. Lett. **78** (1997) 4335 [arXiv:hep-ph/9611320].
33. A. C. Kraan, J. B. Hansen and P. Nevski, Eur. Phys. J. C **49** (2007) 623 [arXiv:hep-ex/0511014].
34. C. Driouichi, Doctoral Thesis, Lund (2004).
35. G. Aad *et al.* [ATLAS Collaboration], JINST **3** (2008) S08003.
36. S. Hellman, M. Johansen and D. Milstead, ATL-PHYS-PUB-2006-015.
37. J. R. Ellis, A. R. Raklev and O. K. Øye, JHEP **0610**, 061 (2006) [arXiv:hep-ph/0607261].
38. M. Kazana, G. Wrochna, P. Zalewski, CMS-CR-1999-019.
39. The CMS Collaboration, CMS-PAS-EXO-08-003.
40. J. Chen, CMS-CR-2008-009.
41. J. L. Pinfold [MOEDAL Collaboration], Nucl. Phys. Proc. Suppl. **78** (1999) 52.
42. J. L. Feng and B. T. Smith, Phys. Rev. D **71** (2005) 015004 [Erratum-ibid. D **71** (2005) 019904] [arXiv:hep-ph/0409278].
43. A. De Roeck, J. R. Ellis, F. Gianotti, F. Moortgat, K. A. Olive and L. Pape, Eur. Phys. J. C **49** (2007) 1041 [arXiv:hep-ph/0508198].
44. K. Hamaguchi, M. M. Nojiri and A. de Roeck, JHEP **0703** (2007) 046 [arXiv:hep-ph/0612060].
45. A. Arvanitaki, S. Dimopoulos, A. Pierce, S. Rajendran and J. G. Wacker, Phys. Rev. D **76** (2007) 055007 [arXiv:hep-ph/0506242].
46. V. M. Abazov *et al.* [D0 Collaboration], Phys. Rev. Lett. **99** (2007) 131801 [arXiv:0705.0306 [hep-ex]].
47. W. Buchmuller, K. Hamaguchi, M. Ratz and T. Yanagida, Phys. Lett. B **588** (2004) 90 [arXiv:hep-ph/0402179].